JOURNAL OF MATERIALS SCIENCE 20 (1985) 421–430

Interfacial effects in carbon-epoxies

Part 1 *Strength and modulus with short aligned fibres*

A. R. SANADI, M. R. PIGGOTT
Department of Chemical Engineering and Applied Chemistry, University of Toronto, Toronto, Ontario M5S 1A4, Canada

Carbon fibre-reinforced epoxy resin samples made with aligned fibres, with lengths of 1 to 5 mm, had strengths and Young's moduli that were affected by fibre length, and surface condition and well as fibre volume fraction. Stress–strain trajectories were all linear, except when the fibres were coated with silicone resin. Fibre critical lengths were found to be affected by the surface condition, but composite strength could not be accounted for when the critical length was inserted into the usual equations, based on fibre slip. The results indicate that existing theoretical treatments for strength and modulus should take more account of the overstressing of fibres adjacent to fibre ends.

1. Introduction

The processes that take place at the interface between fibres and matrix are of fundamental importance for fibre composites. This is because stress transfer between the matrix, and the fibres, which normally carry most of the load, takes place there. Thus the interface controls most of the mechanical properties of the composite, e.g. strength, Young's modulus, etc.

When the fibres are aligned, and very long compared to their diameters, as in structures made from prepreg tapes, the interface has only very little effect on the strength and the Young's modulus of the composite in the fibre direction, although a weak interface can drastically reduce off-axis strengths, flexural strength [1] and compression strength [1, 2].

With short fibres, on the other hand, the interface does have a significant effect on tensile strength and Young's modulus [3], and curved stress–strain trajectories have been observed [3,4], although it should be noted that, in the earlier paper, the whole stress–strain trajectory was curved, while in the later one, a straight trajectory was reported up to 0.5% strain. Water has a drastic effect on the interface; it reduced the modulus by nearly 80% and the strength by 70% when the fibres were not sized [5]. All these short-fibre experiments were carried out with thermoplastics. With thermosets, reinforced by short aligned fibres, curved stress–strain trajectories have also been observed [6].

A simple treatment, using a single fibre-matrix tube model to represent the composite, predicts continuously curved stress–strain trajectories, when slip can occur at the interface, due to matrix yielding, or to frictional sliding ([7], Ch. 4). If interface yielding or fracture precedes slip, the stress–strain trajectory has a linear region [8], terminating at a strain, ϵ_{1s}, given approximately [9] by

$$\epsilon_{1s} = a\sigma_{mu}(E_f E_m)^{1/2}, \quad (1)$$

where a is a dimensionless parameter indicating the tenacity of the bond between fibres and matrix, and equal to 1.00 when the bond strength is equal to the matrix strength, σ_{mu}. E_f and E_m are fibre and matrix Young's moduli. (The 0.5% critical strain for slip [4] corresponds to $a = 1.7$, or a maximum shear stress at the interface of 60 MPa.)

In the elastic region, before slip starts, the interface is not expected to influence the Young's modulus of the composite in the fibre direction [8], although the length of the fibres will influence the modulus significantly. Thus, theory and experiment are not in complete agreement. This investigation was designed to study these effects in a consistent and planned fashion with controlled interface properties, and with fibre length and volume fraction as variables, having pre-selected

0022–2461/85 $03.00 + .12

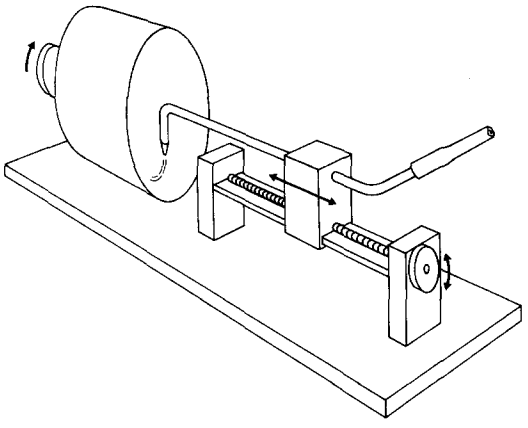

Figure 1 Schematic diagram of aligning system.

values. Fibre critical lengths were measured using established techniques [10].

2. Experimental method

Union Carbide pitch precursor P-55S fibres were used in this work. They were cut to lengths of 0.5, 1, 2, 3 and 5 mm. As-received, they were sized. Before use, some were desized using a 1:1 methyl ethyl ketone–propanol mixture. Others were desized and then etched with 70% nitric acid for 6 h, and still others were coated with silicone oil (Dow Corning 200).

The resin matrix was Shell Epon 815, with 19% Ancamine 1482 added as hardener. The resin was cured at 100° C, and then post-cured at 160° C for 4 h.

To make the composites, aligned fibre mats were made by suspending the fibres in glycerine, and then allowing the mixture to flow through a tube, with a tapered end, on to a rotating drum [11]. Fig. 1 is a schematic drawing of the process. The fibres were aligned as they passed through the nozzle, and an aligned fibre mat was produced, on the mesh inside the drum, while the glycerine passed through the mesh.

The mats were washed, then impregnated with resin, and moulded under a pressure of 0.7 MPa. The pressure was not applied until the resin had gelled. Test coupons were cut from the moulds, end tabbed, and tensile tested using an Instron machine with an extensometer for measuring the strains. The cross-head speed was 0.5 mm min^{-1}. Izod impact tests were also carried out.

Single fibres were embedded in the resin. The "composite" was then extended to a strain of 0.8% (the breaking strain of the fibre was 0.50%). The lengths of the fibre fragments resulting from this were measured *in situ*, using a microscope, and were also measured after digesting the matrix in a mixture of equal proportions of concentrated nitric and sulphuric acids.

Fibre length measurements were also carried out on the aligned fibre composites. The matrix was burned off at 400° C for this. In addition, fibre orientation was determined by measuring the angles of 200 fibres in the mats, using a microscope.

3. Experimental results

By careful setting of the nozzle, it was possible to get 60% of the fibres within 5° of the alignment direction, Fig. 2, except for the 0.5 mm long fibres. (The 0.5 mm fibres were not used to make composites.)

Some breakage of fibres occurred during the various processing steps. Initially, all fibres had lengths within ± 0.05 mm of the desired length. The processing caused some breakage of the fibres. Fig. 3 shows the cumulative number of fibres against observed length for the 1, 2, 3 and 5 mm fibres taken from composites with a fibre volume fraction, V_f, of 0.35. If we assume only two fragments for each broken fibre, then these distributions indicate about 17% breakage for the 3 and 5 mm, fibres, 15% breakage for the 2 mm fibres, and 13% for the 1 mm fibres. The corresponding figures for fibres extracted from a composite with $V_f = 0.2$ are: 5 mm, 13%; 3 and 2 mm, 12%; and 1 mm, 9%.

The Young's moduli of the 2 and 5 mm fibre composites were linear functions of fibre volume fraction, Figs. 4 and 5. Thus they obeyed a modified rule of mixtures expression:

$$E_1 = A_E V_f E_f + V_m E_m, \qquad (2)$$

where E_1 is the composite Young's modulus in the fibre direction. $V_m = 1 - V_f$, and A_E is a modulus reduction factor dependent on fibre length and orientation, etc. (For perfectly aligned continuous fibres we expect $A_E \simeq 1.00$.)

A_E was affected by the fibre surface treatment, although the difference between desizing and etching was only apparent with the 5 mm fibres, Fig. 5. The silicone coated fibres gave composites with moduli that were less then half those obtained with sized fibres. The modulus (and hence A_E) was also affected by the fibre length, Fig. 6. With silicone-coated fibres, there appeared to be little increase in modulus for fibre lengths

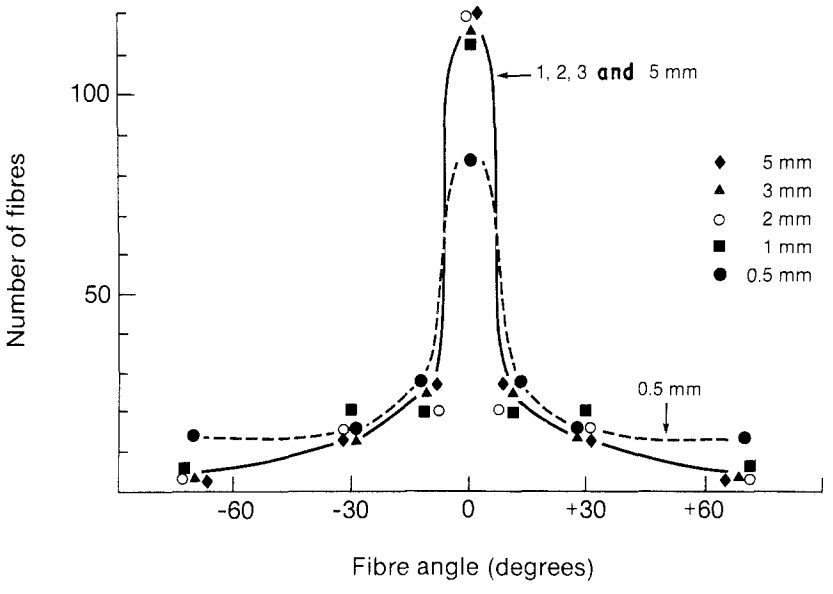

Figure 2 Angular distribution of fibres.

greater than 2 mm, while with the sized fibres the modulus increased continuously with fibre length.

The strengths of the composites increased montonically with fibre volume fraction, Figs. 7 and 8, and in some cases had approximately linear regions from $V_f = 0.15$ to 0.25. It is usual to assume that a modified rule of mixtures expression can be used for strength, σ_{lu}, as well as modulus;

$$\sigma_{lu} = A_s V_f \sigma_{fu} + V_m E_m \sigma_{fu}/E_f \qquad (3)$$

where σ_{fu} is the fibre strength, and A_s is the strength reduction factor for misaligned and short fibres, etc. Since the composites had breaking strains which were less than the matrix breaking strain of about 2.3% (see Fig. 10) we have assumed a matrix contribution to strength corresponding to failure at the fibre breaking strain, $\epsilon_{fu}(= \sigma_{fu}/E_f)$. The dashed lines in Figs. 7 and 8 were drawn to intersect the strength axis at $E_m \epsilon_{fu}$. It is clear that Equation 2 only governs a small part of the behaviour of these composites.

Fibre length had little effect on composite strength, for lengths greater than about 2 mm, Fig. 9. The effect of fibre length was greater at the higher fibre volume fraction, however.

Except for the composites made with silicone-coated fibres, the stress–strain trajectories of all the composites were linear to failure. Fig. 10 shows the composite breaking strains. In this figure, the fibre lengths (in mm) are given by the numbers on the graph. The shape surrounding the numbers indicates the surface treatment; an

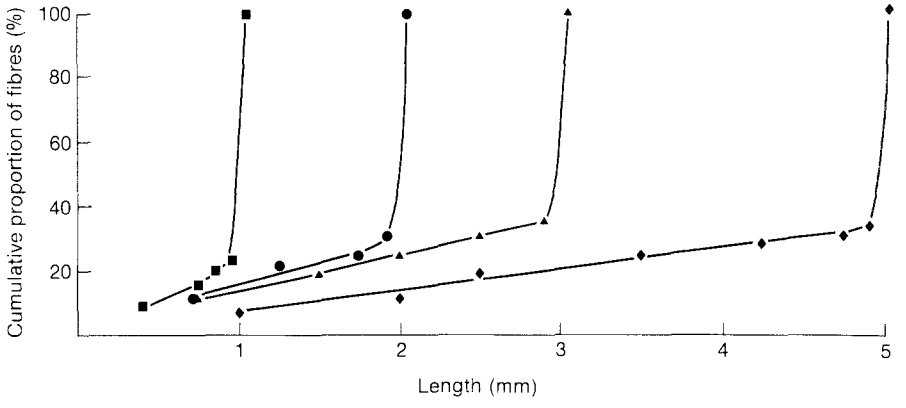

Figure 3 Cumulative distribution of fibre lengths, $V_f = 0.35$.

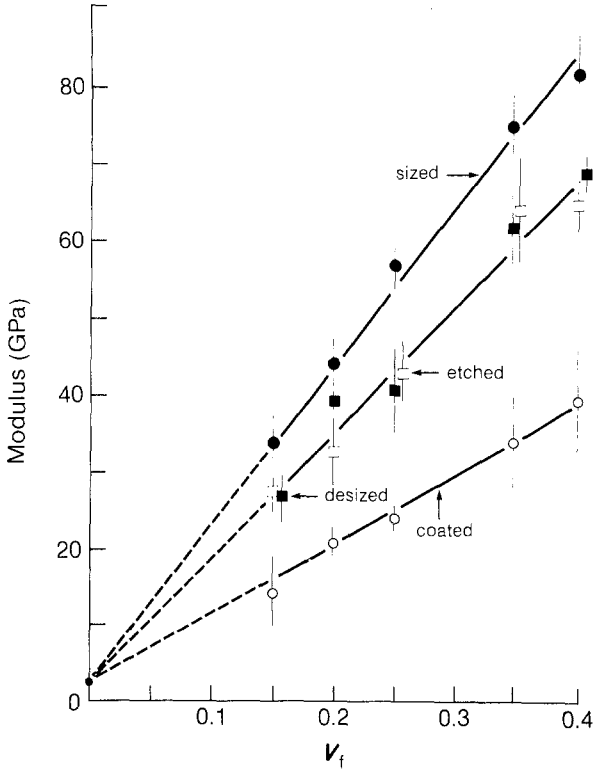

Figure 4 Young's moduli of composites made with 2 mm long fibres.

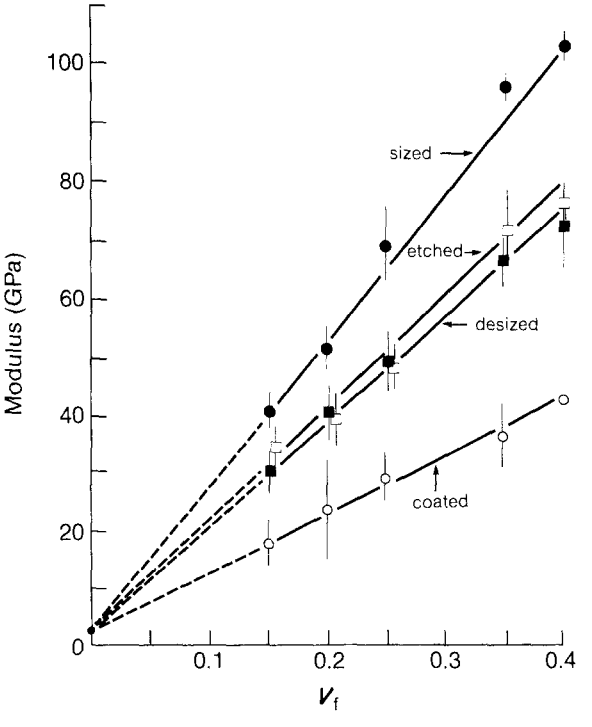

Figure 5 Young's moduli of composites made with 5 mm long fibres.

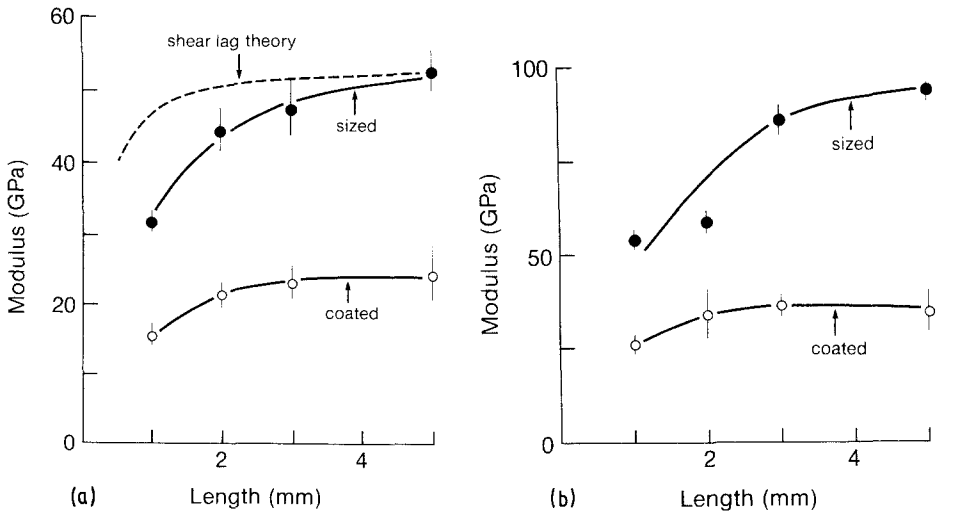

Figure 6 Effect of fibre length on Young's moduli of composites with, (a), $V_f = 0.20$ and, (b), $V_f = 0.35$.

inverted triangle for the sized fibres and a square for the silicone-coated fibres. A curved stress–strain strain trajectory is indicated by a circle within the shape.

The composite breaking strains were close to the fibre breaking strains when the fibres were sized, but decreased with increasing fibre volume fraction. For the 1 mm sized fibres the composite breaking strains were less than those with the 2, 3 and 5 mm sized fibres. The composite breaking strains were greater for the silicone-coated fibres, and increased with decreasing fibre volume fraction, so that, at $V_f = 0.15$ and 0.2, they were more than $2\epsilon_{fu}$ and greater than half the matrix breaking strain, $\epsilon_{mu}/2$. Fibre length appeared to have no consistent effect on the breaking strain of the composites when the fibres were coated.

Fig. 11 shows a typical curved stress–strain trajectory. This was from a composite made with 2 mm silicone coated fibres with $V_f = 0.2$. Note the stress plateau region.

The fibre critical lengths are shown in Fig. 12.

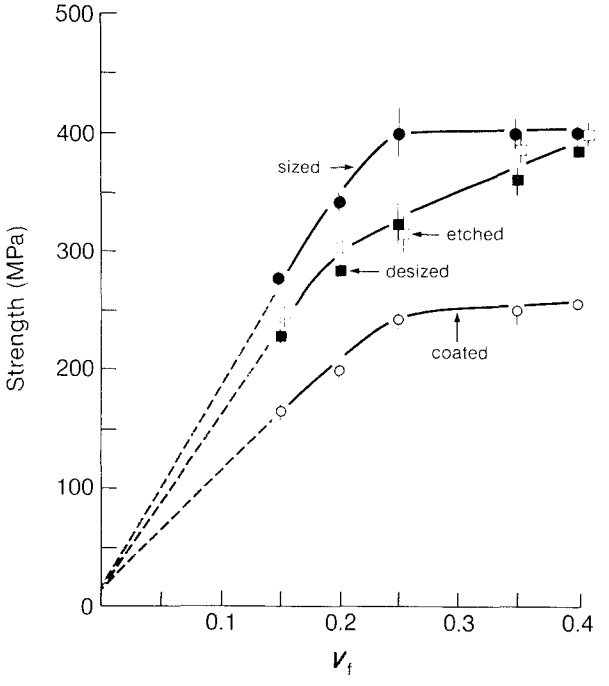

Figure 7 Tensile strengths of composites made with 2 mm long fibres.

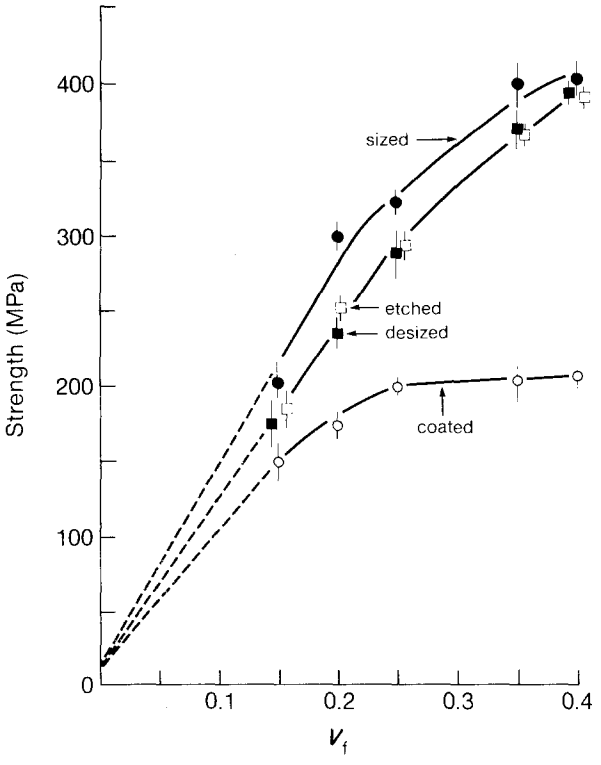

Figure 8 Tensile strengths of composites made with 5 mm long fibres.

The silicone coating more than doubled the critical length, but the other surface treatments had little effect.

4. Discussion

As indicated in Section 1, slip theory is commonly used to explain the failure of short-fibre composites. Associated with the slip, between matrix and fibres, we expect a reduction in composite strength, and a curved stress–strain trajectory. Prior to the onset of slip, the stress–strain trajectory, should be straight, and some slight reduction in Young's modulus should be observed [8] due to "shear lag", (The Young's modulus is usually estimated from one of the many shear lag models available.)

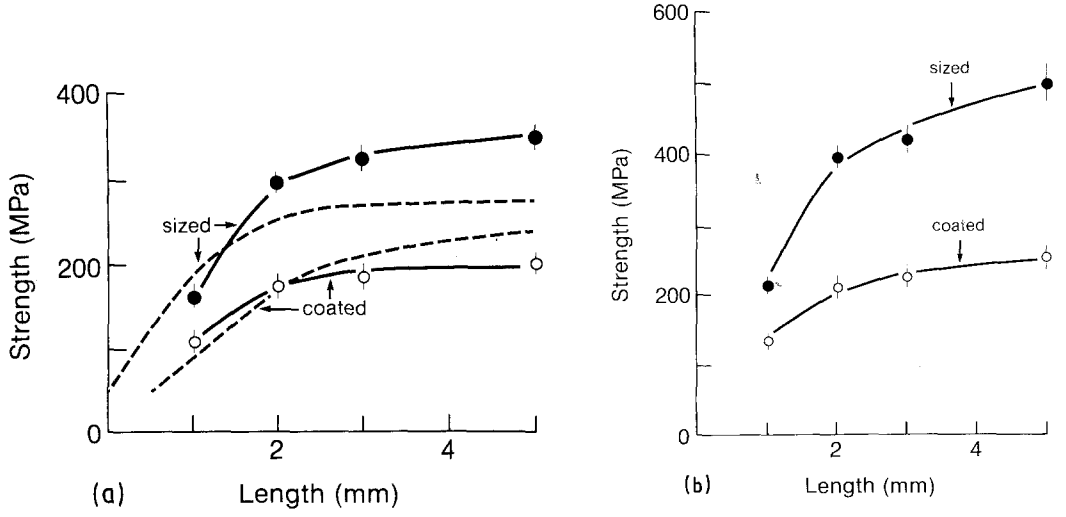

Figure 9 Strength plotted against fibre length, (a) $V_f = 0.20$ and (b), $V_f = 0.35$. The dashed lines are the theoretical curves using simple slip theory.

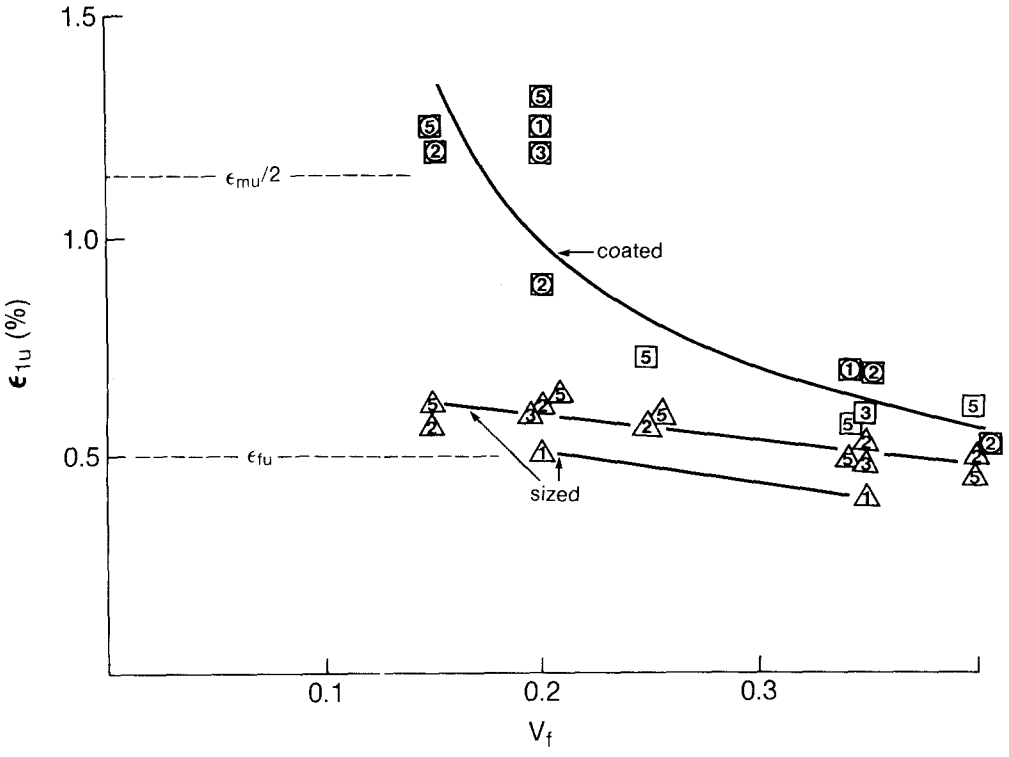

Figure 10 Breaking strains of composites. Fibre length is indicated by figure on graph. Square and triangular shapes indicate silicone-coated and sized fibres, respectively. Circle indicates curved stress–strain trajectory.

In these experiments, most stress–strain curves were linear to failure, yet very significant reductions in modulus were observed. In order to determine what part shear lag and slip may have played in the results, we will first examine the results using modified rule of mixtures expressions.

For modulus we will use

$$E_1 = \chi_1 \chi_2 V_f E_f + V_m E_m, \quad (4)$$

where χ_1 is a fibre alignment factor and χ_2 is a fibre length factor. It is assumed that these two effects operate independently in this way [4]. In our experiments, Equation 2 was obeyed. If theory and experiment agreed, we would expect, comparing Equations 2 and 4, that

$$A_E = \chi_1 \chi_2. \quad (5)$$

Since our fibres were not perfectly aligned, we expect χ_1 to be less than 1. To estimate χ_1 we

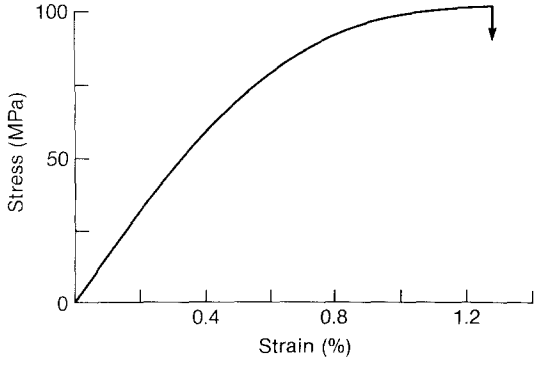

Figure 11 Stress–Strain curve. 1 mm long silicone-coated fibres, $V_f = 0.20$.

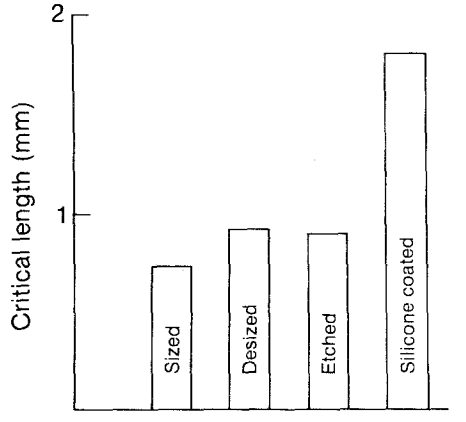

Figure 12 Fibre critical lengths.

TABLE I Constants governing strength and modulus against fibre volume fraction plots

Fibre length (mm)	Surface treatment	Modulus constants				Strength constants				$A_s/\chi_3\chi_4$ (%)
		Expt. A_E (%)	χ_1	χ_2	$\chi_1\chi_2$	Expt. A_s (%)	χ_3	χ_4	$\chi_3\chi_4$	
2	sized	58	0.67	0.93	0.62	74	0.74	0.80	0.59	125
	desized	44				61		0.75	0.56	109
	etched	44				61		0.76	0.56	109
	coated	25				46		0.51	0.38	121
5	sized	67	0.68	0.97	0.66	92	0.76	0.92	0.70	131
	desized	52				79		0.90	0.68	116
	etched	59				79		0.90	0.68	116
	coated	28				55		0.79	0.60	132

divide the composite into laminae containing fibres in different orrientation, ϕ: ± 2.5°, ± 10°, ± 30°, ± 67.5°, and estimate the modulus, E_ϕ, for each lamina, according to the expression

$$\frac{1}{E_\phi} = \frac{\cos^4\phi}{E_1} + \left(\frac{1}{G_{12}} - \frac{2\nu_{12}}{E_1}\right) \times \sin^2\phi\cos^2\phi + \frac{\sin^4\phi}{E_2}. \quad (6)$$

Here E_2 is the Young's modulus normal to the fibre direction, G_{12} is the shear modulus and ν_{12} is the Poisson's ratio. We use $E_1 = V_f E_f + V_m E_m$, $1/E_2 = V_f/E_f + V_m/E_m$, $1/G_{12} = V_f/G_f + V_m/G_m$ and $\nu_{12} = V_f\nu_f + V_m\nu_m$, where subscripts f and m indicate fibre and matrix values of shear modulus and Poisson's ratio. (These are the moduli calculated on the basis of series (E_1 and ν_{12}) and parallel (E_2 and G_{12}) fibre arrangements ([7], Ch. 4); although E_2 and G_{12} are very approximate, they should be adequate for this purpose). We will use $V_f = 0.3$ for this calculation, since this is about in the middle of the V_f range where Equation 2 fits the results. The relative thickness of each lamina, t, is given by the relative number of fibres in the range of angles corresponding to each ϕ value, and is shown in Fig. 2. The values of χ_1 is given by

$$\chi_1 = \sum_{k=1}^{4} E_{\phi k} t_k / E_1 \sum_{k=1}^{4} t_k. \quad (7)$$

χ_1 values, so calculated, are given in Table I.

χ_2 may be estimated from shear lag theory (see e.g. Cox [12]). The appropriate expression is:

$$\chi_2 = 1 - \tanh(ns)/ns \quad (8)$$

where

$$n^2 = 2Em/E_f(1+\nu_m)\ln(P_f/V_f), \quad (9)$$

s is the fibre aspect ratio, and P_f is the fibre packing factor equal to $(2\pi/3^{1/2})$ for hexagonally packed fibres. In the range $V_f = 0.15$ to 0.40 n varies between 0.054 and 0.065. Since the minimum fibre aspect ratio is about 100, $\tanh(ns)$ is always extremely close to 1.00 and we can write

$$\chi_2 = 1 - 1/ns. \quad (10)$$

Thus χ_2 varies between 0.926 and 0.938 for the 2 mm fibres, according to the fibre volume fraction, and 0.970 and 0.975 for the 5 mm fibres. We will use 0.93 and 0.97 for χ_2 (Table I).

Comparing the product $\chi_1\chi_2$ with A_E in Table I, we see that the agreement is quite good for the 5 mm long sized fibres, but gets progressively less good with surface treatments that increase the critical fibre length. Also, with the sized fibres, the effect of fibre length is much greater than indicated by the shear lag theory. Thus the agreement between $\chi_1\chi_2$ and A_E is less good for the 2 mm fibres than the 5 mm fibres (Table I), and, while about an 11% increase should be observed (Equation 10) going from the 1 mm to 5 mm fibre length, the effect actually observed, Fig. 6, is a 71% increase. (The dashed line in Fig. 6, upper graph, shows the shear lag prediction for $V_f = 0.20$.) Thus the modulus results do not fit the shear lag theory, at least in the simple form proposed by Cox.

For strength we will use

$$\sigma_{1u} = \chi_3\chi_4\nu_f\sigma_{fu} + V_m E_m \epsilon_{fu}, \quad (11)$$

where χ_3 is the fibre direction factor and χ_4 the fibre length factor. If theory and experiment agree,

$$A_s = \chi_3\chi_4. \quad (12)$$

We derive χ_3 using the same method as used for χ_1, except that, for strength, we use the expression:

$$\frac{1}{\sigma^2_{u\phi}} = \frac{\cos^4\phi}{\sigma^2_{1u}} + \left(\frac{1}{\tau^2_{12u}} - \frac{1}{\sigma^2_{1u}}\right) \times \cos^2\phi\sin^2\phi + \frac{\sin^4\phi}{\sigma_{2u}}. \quad (13)$$

Here $\sigma_{u\phi}$ corresponds to the composite strength at an angle ϕ to the fibre direction. $\sigma_{1u} \simeq V_f\sigma_{fu} + V_m E_m \epsilon_{fu}$, τ_{12u} is the shear strength of the composite which we will assume is equal to half the tensile strength of the matrix, and σ_{2u} is the tensile strength of the composite normal to the fibres, which we will assume to be equal to the matrix strength. We estimate σ_{1u} at $V_f = 0.15$, since Equation 3 is obeyed (if at all) only at low fibre volume fractions.

$$\chi_3 = \sum_{k=1}^{4} \sigma_u \phi_k t_k / \sigma_{1u} \sum_{k=1}^{4} t_k \qquad (14)$$

values of χ_3 are given in Table I.

We use slip theory to estimate χ_4:

$$\chi_4 = 1 - s_c/2s \qquad (15)$$

where s_c is the critical fibre aspect ratio. Using the values for L_c given in Fig. 12 we obtain the χ_4 values listed in Table I. (Note that s_c/s is the same as the ratio of the critical fibre length to the actual fibre length.)

Comparing A_s and the product $\chi_3\chi_4$ we notice that the slip theory produces too low a value in all cases: the experiments produce results that range from 9% higher to 32% higher than theory would indicate. Also, the effect of fibre length is greater than expected for the sized fibres, and less than expected for the silicone-coated fibres. Thus, at $V_f = 0.2$, going from the 1 to 5 mm length we expect (Equations 10 and 14) a 44% increase in strength while a 123% increase is actually observed for the sized fibres. With the silicone-coated fibres, we expect about a 50% increase going from the 2 mm to the 5 mm fibre length, while the experiments indicated almost no increase at all. (Note that, for the 1 mm fibre length in the silicone-coated case, the length is less than the critical length; in this case $\chi_4 = s/2s_c$.) The slip theory predictions are shown, for comparison, in Fig. 9, for $V_f = 0.2$.

Neither the modulus results, nor the strength results can be fitted into the theories used at present, at least in their simple forms. As noted in Section 1, lower than expected Young's moduli have been observed previously, and Lees [13] has provided an empirical formula which can be fitted to some of the results.

It seems most unlikely that elasticity solutions will be very useful in this context, since the central role played by the interface suggests that some type of failure, together with slip, is taking place, almost as soon as any stress is applied. Matrix cracking, initiated by the stress concentrations at the fibre end, has been observed with reinforced thermoplastics, see e.g. Bader and Collins [5], and analysed in a number of different ways by Chou and co-workers, see e.g. Manders and Chou [14]. These, and other probabilistic theories (see e.g. Rosen [15]) have given useful insight into failure processes, but are less helpful in explaining modulus losses through interface weakness.

An alternative approach, first explored by Riley [16], may be more fruitful. This considers the extra stresses imposed on fibres adjacent to a fibre end, and predicts some loss in strength. (Chou and co-workers also takes account of this.) Recently [17], the effect of this on the modulus and stress–strain curve has been examined, but so far taking no account of fibre slip. Stress–strain trajectories with a linear region at low strain and a curved region just below the matrix yield strain were predicted in a two-dimentional model, appropriate for platelets. The curved region started at a strain where matrix yielding between the platelets, adjacent to platelet ends, became significant. Experiments with steel platelet-reinforced polycarbonate gave linear stress–strain trajectories up to failure [18], but are not in conflict with this model because of the low failure strain of the composite. With appropriately packed platelets, slip theory, in the absence of significant matrix yielding, predicts linear stress–strain trajectories ([7], Ch. 8).

This approach can account for the results obtained here, qualitatively at least, as follows. The extra stresses in the regions of fibres adjacent to a fibre end signify larger local strains in these regions. Hence the compliance of the composite is increased by the presence of these fibre ends, and thus the Young's modulus is reduced. If the critical length of the fibre is large (i.e. the interfacial slip stress is small) the regions of extra stress will be more extended than if the fibre critical length is small. This implies a linear relationship between compliance and fibre critical length. Hence the modulus should decrease with increasing fibre critical length.

The effect on the strength of the composite of this overstressing of the fibres is more difficult to deal with, Riley notwithstanding. This is because, in carbon (and glass and boron) fibre composites, the fibres are brittle, with strengths controlled

by flaws. If the overstressed region of the fibre does not contain a flaw, it should not fail. This problem can be solved, in principle at least, by assuming some flaw distribution in the fibres [15], but in practice, the only data we have are strength–length relationships; these are available for glass [19] and carbon [20]. They show two regions, governed by different constants, A and m, in the equation

$$\sigma_{fu} = AL^{-m},$$

where L is the fibre length. Thus, more than one flaw distribution is needed. Note that a graphical method has been proposed which avoids this problem ([7], p. 120). The non-linear variation of composite strength with fibre volume fraction could be due to the reduced "cushioning" effect of the matrix, at high fibre volume fractions, leading to a decrease in strength, through a transfer of stress to fewer adjacent fibres.

5. Conclusions

Short aligned fibre composites have lower moduli and strengths than expected theoretically. The variation of modulus with fibre length does not agree with predictions based on shear lag theory. In addition, with the exception of the silicone-coated fibres, the stress–strain curves were linear, indicating that the slip process that takes place with reinforced thermoplastics [3] and gives curved stress–strain trajectories, was not taking place unless the fibres were extremely poorly bonded. In any case the strength results could not be fitted to the simple slip theory either. However, if account is taken of fibre overstressing adjacent to a fibre end, the results can be explained qualitatively on the basis of fibre slip.

Acknowledgements

The authors are grateful to Hartford Fibres, Kingston, Ontario, for cutting the fibres, and the Industrial Materials Research Institute (DSS contract no. 09SD-31155-1-5001) for financial support for this work.

References

1. L. J. BROUTMAN, *Poly. Eng. Sci.* **6** (1966) 1.
2. N. L. HANCOX, *J. Mater. Sci.* **10** (1975) 234.
3. W. H. BOWYER and M. G. BADER, *ibid.* 7 (1972) 1315.
4. P. T. CURTIS, M. G. BADER and J. E. BAILEY, *ibid.* **13** (1978) 377.
5. M. G. BADER and J. F. COLLINS, Proceedings of ICCM4, Tokyo, October 1982, edited by T. Hayashi, K. Kawata and S. Umekawa (Japan Society for Metals, Tokyo, 1982) p. 1067.
6. O. ISHAI and R. E. LAVENGOOD, 24th ANTEC, SPI (1969) 11F.
7. M. R. PIGGOTT, "Load Bearing Fibre Composites" (Pergamon, Oxford, 1980).
8. *Idem, J. Mater. Sci.* **13** (1978) 1709.
9. *Idem, Polymer Composites* **3** (1982) 179.
10. J. D. HUGHES, AERE R 8683 (1977).
11. H. EDWARDS and N. P. EDWARDS, Proceedings of ICCM3, Paris, August 1980, edited by A. R. Bunsell, A. Martrenchar, D. Menkes and G. Vercherry (Pergamon Press, Oxford, 1980) p. 1620.
12. H. L. COX, *Brit. J. Appl. Phys.* **3** (1952) 72.
13. J. K. LEES, *Polymer Eng. Sci.* 8 (1968) 186.
14. P. W. MANDERS and T. W. CHOU, Proceedings of ICCM4, Tokyo, October 1982, edited by T. Hayashi, K. Kawata and S. Umekawa (Japan Society for Metals, Tokyo, 1982) p. 1075.
15. B. W. ROSEN, *AIAA J.* **2** (1964) 1985.
16. V. R. RILEY, *J. Comp. Mater.* 4 (1968) 436.
17. B. SCHULTRICH, W. POMPE and H. J. WEISS, *Fibre Sci. Tech.* **11** (1978) 1.
18. B. GLAVINCHEVSKI and M. R. PIGGOTT, *J. Mater. Sci.* 8 (1973) 1373.
19. A. G. METCALF and G. K. SCHMITZ, *ASTM Proc.* 64 (1974) 1075.
20. J. W. HITCHON and D. C. PHILLIPS, AERE R 9132 (1978).

Received 27 February
and accepted 12 March 1984